

Construction of 2D layered BiVO₄/Zinc Porphyrin (ZnTCPP) S-scheme heterostructure boosting photocatalytic N₂ oxidation performance

Desen Zhou^a, Shuai Shao^a, Xuan Zhang^a, Tingmin Di^b, Jun Zhang^{a,}, Tielin Wang^{a,*},*

Cunwen Wang^a

a Key Laboratory of Green Chemical Process of Ministry of Education, Key Laboratory of Novel Reactor and Green Chemical Technology of Hubei Province, School of Chemical Engineering and Pharmacy, Wuhan Institute of Technology, Wuhan 430205, P. R. China.

b School of Materials Science and Engineering, Wuhan Institute of Technology, Wuhan 430205, P. R. China

*Corresponding author.

E-mail address: junzhang@wit.edu.cn (J. Zhang); witwangtl@hotmail.com (T. L. Wang)

Experimental Section

Synthesis of ultrathin BiVO₄ nanosheets: In a typical synthesis, 7 mmol of BiCl₃ and 2.88 mmol cetyltrimethyl ammonium bromide (CTAB) were dissolved in 60 mL of ethylene glycol (EG), the emulsion was obtained with stirring more than 40 min. After that 7 mmol of Na₃VO₄ was slowly added under drastic stirring for another 60 min. Then the yellow mixture was transferred into a 100 mL Teflon-lined autoclave, sealed and heated at 160 °C for 3 hours. The product was cooled to room temperature naturally and then washed with water and ethanol for several times, then air dried at 80 °C for 12 hours.

Synthesis of ZnTCPP nanosheets: First, accurately weigh 8 mg of pyrazine, 45 mg of Zn(NO₃)₂, 200 mg of PVP and 40 mg of TCPP, and then add them to 60 mL of a mixed solution of DMF:ethanol=3:1 (v:v) in an oil bath. After refluxing at 80 °C for 16 h, the product was washed several times with absolute ethanol and DMF.

Synthesis of 2D/2D BiVO₄/ZnTCPP composites: The 2D/2D BiVO₄/ZnTCPP composites were prepared by a reflow method and illustrated in Scheme 1. Typically, 0.1 g of BiVO₄ and a certain amount of ZnTCPP were added to 100 mL ethanol solution, and the solution was refluxed at 50 °C for 12 h. The nominal weight contents of ZnTCPP in the composite materials were 0%, 10%, 20%, and 50%, respectively, and the corresponding samples were marked as BVO, BZ-10, BZ-20 and BZ-50.

Characterization: The crystalline phases of the obtained samples were recorded on X-ray diffraction (XRD) by an X-ray diffractometer (Rigaku, Japan) using Cu K_α radiation ($\lambda = 0.15418$ nm) at a scan rate (2θ) of 0.05° s⁻¹. The morphology of the

samples was characterized by field emission scanning electron microscopy (FESEM) on JSM-7500 electron microscope (JEOL, Japan) operating at an accelerating voltage of 15 kV. Morphological observation was further visualized by the transmission electron microscopy (TEM) on a Tecnai G² F20 S-TWIN microscope with a field emission gun at a 200 kV accelerating voltage. The thickness of the samples was tested by atomic force microscopy (AFM, Bruker Dimension Icon). UV-vis diffuse reflectance spectra were investigated by a UV-vis spectrophotometer (UV-2600, Shimadzu, Japan) using BaSO₄ powder as a reference standard. The Brunauer-Emmett-Teller (BET) surface area was carried by Micromeritics ASAP 2020 nitrogen adsorption apparatus (USA). All the samples were degassed at 150 °C before nitrogen adsorption measurements. The BET specific surface area was tested by a multipoint BET method using the adsorption data in the relative pressure (P/P_0) range of 0.05-0.25. The pore size distributions were measured utilizing desorption data by the Barrett-Joyner-Halenda (BJH) method. The pore volume and average pore size was determined by the nitrogen adsorption volume at the relative pressure (P/P_0) of 0.972. X-ray photoelectron spectroscopy (XPS) measurements were operated by an ultra-high-vacuum VG channel detector. The spectra were excited using Al K_α (1486.7 eV) radiation (operated at 300 W) of a twin anode in the constant analyzer energy mode with an energy of 30 eV. Time-resolved fluorescence emission spectra were surveyed by a FLS920 fluorescence lifetime spectrophotometer (Edinburgh Instruments, UK) with the excitation of 375 nm and the detection wavelength of 540 nm using silica gel as the reference standard. Surface photovoltage (SPV) spectra were measured by a 350

W xenon lamp, and the scanning wavelength range is 300-600 nm (PL-SPS/IPCE 1000 Beijing Perfect Light Technology Co., Ltd).

Photoconversion of N₂ into nitrate: A 100 mL quartz three-necked flask was used as the photoreactor for photocatalytic reaction at ambient temperature and atmospheric pressure. Before the measurement, the catalysts were washed by ultrapure water in order to avoid the disturbing of other ions. After that 0.1 g of catalysts were dispersed in 60 mL ultrapure water by ultrasonic treatment. In the experiment process, a mixture of ultrapure N₂ (99.999%) and ultrapure O₂ (99.995%) (3:1/v:v) was purged into the solution for 30 min in the dark. A 300 W Xe arc lamp through a UV-cutoff filter (≤ 420 nm) was used as visible-light source. The concentration of NO₃⁻ and NO₂⁻ were tested after 3h irradiation using an ion chromatograph (IC1010, Techcomp). The concentration of NO₂⁻ was found to be negligible, which suggested that during the photocatalytic NOR reaction, NO₃⁻ was the main product by oxidation of NO in the presence of O₂ and H₂O.

The apparent quantum efficiency (QE) under monochromatic light irradiation was determined using single wavelength filters with a bandwidth of ± 5 nm. The details of the QE calculation are shown as follows:

QE(%)=100×(number of molecules nitrate generated×5)/number of incident photons

$$=100\times M\times N_A\times 5/(I\times A\times t\times \lambda/hc)$$

Where M represents the amount of nitrate generation, N_A represents Avogadro's constant, I is the light intensity, A is the light incident area, t is the light incident time, λ is the light irradiation wavelength, h is the Plank constant, and c is speed of light.

Photoelectrochemical measurements: The electrochemical signals were collected by electrochemical workstation (Chenhua CHI660C, China) in a standard three-electrode system. a fluorine-doped tin oxide (FTO) glass coated with ca. 1.0 cm² samples, a Pt wire and an Ag/AgCl electrode were immersed in the electrolyte of 0.5 M Na₂SO₄ solution, corresponding to working electrode, counter electrode and reference electrode, respectively. A 3 W LED (405 nm) was served as light source.

Computational detail: Density function theory (DFT) calculations were performed by using the CP2K-8.1 package. Perdew-Burke-Ernzerh (PBE) of functional was used to describe the system. Unrestricted Kohn-Sham DFT has been used as the electronic structure method in the framework of the Gaussian and plane waves (GPW) way. The Goedecker-Teter-Hutter (GTH) pseudopotentials and Double- ζ molecularly optimized basis sets (DZVP-MOLOPT-GTH) have been used for all elements. A plane-wave energy cutoff of 400 Ry has been employed. The geometries were optimized using the Broyden-Fletcher-Goldfarb-Shanno (BFGS) algorithm, and the convergence criterion for the forces was set to 4.5×10^{-4} bohr/hartree. A vacuum layer of 15 Å was constructed to eliminate interactions between periodic structures of surface models. The van der Waals (vdW) interaction was amended by the DFT-D3 method of Grimme.

Table S1 The corresponding physicochemical properties of the prepared samples.

sample	S _{BET} (m ² ·g ⁻¹)	V _{pore} (cm ³ ·g ⁻¹)	D _{pore} (nm)
BVO	42	0.33	24
ZnTCPP	308	0.31	9
BZ-20	119	0.38	15

Table S2 Time-resolved fluorescence decay data of BVO and BZ-20 samples.

Sample	τ ₁ (ns)	A ₁	τ ₂ (ns)	A ₂	A ₁ ' (%)	A ₂ ' (%)	τ _{ave} * (ns)
BZ-20	2.81	11.72	0.5	2.88	95.81	4.19	2.79
BVO	5.55	0.19	0.5	3.33	38.14	61.86	4.91

* The calculation formula is shown in equation:

$$A_1' = \frac{A_1 \times \tau_1}{A_1 \times \tau_1 + A_2 \times \tau_2} \text{ and}$$
$$\tau_{ave} = \frac{A_1' \times \tau_1^2 + A_2' \times \tau_2^2}{A_1' \times \tau_1 + A_2' \times \tau_2}$$

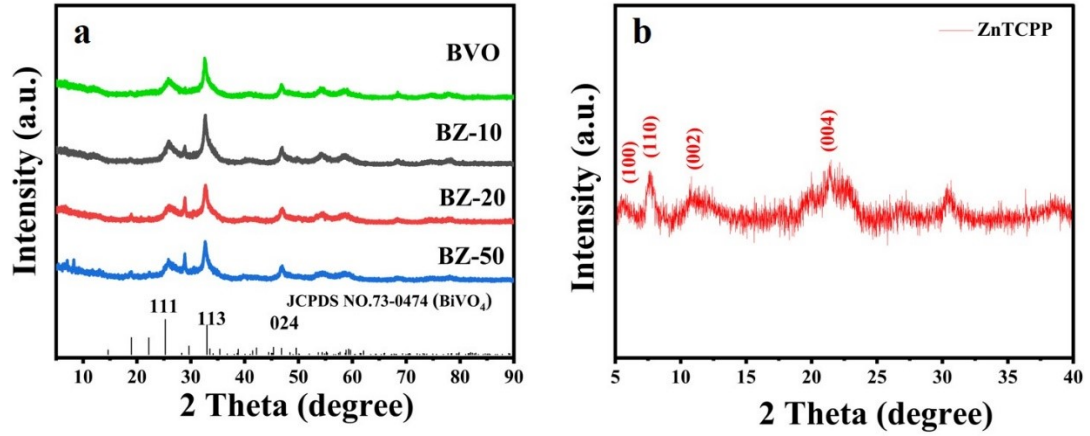


Figure S1. XRD pattern of the prepared ZnTCPP, BVO, BZ-10, BZ-20 and BZ-50 samples.

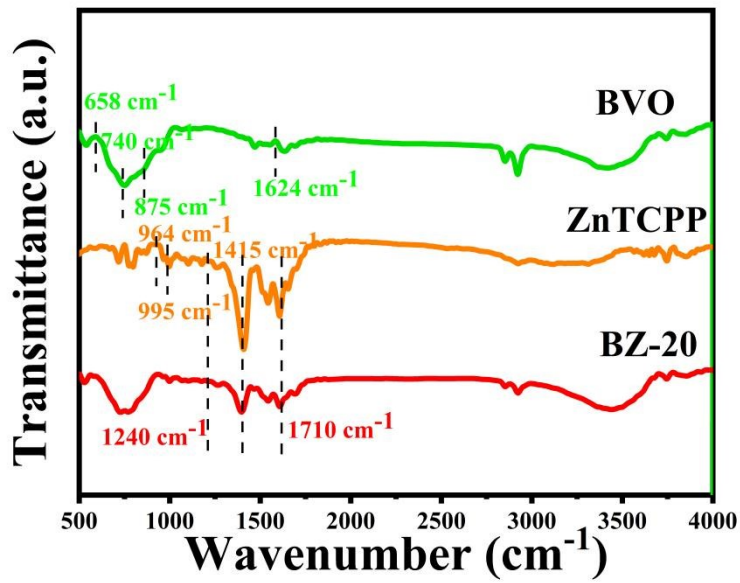


Figure S2. FT-IR pattern of the BVO, ZnTCPP and BZ-20 samples.

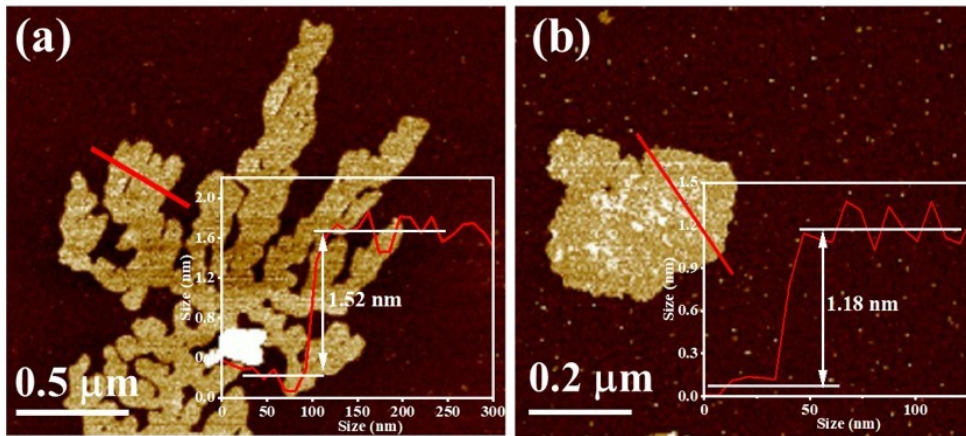
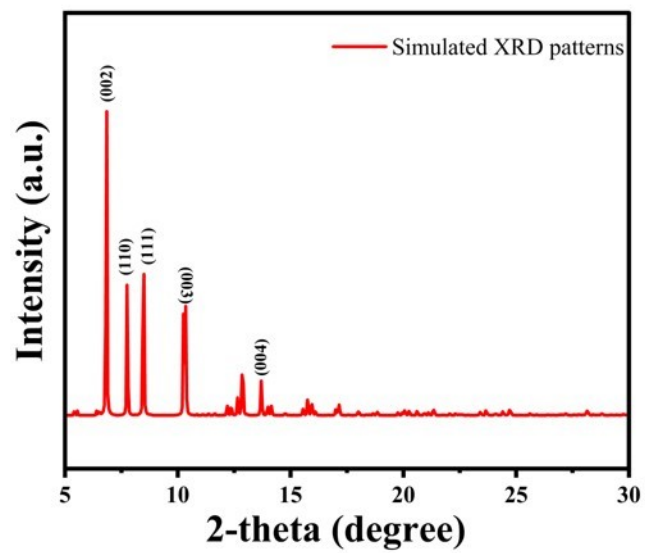


Figure S3. AFM images and the corresponding height profiles of (a) BiVO_4 and (b)



ZnTCPP nanosheets.

Figure S4 The simulated XRD patterns of ZnTCPP.

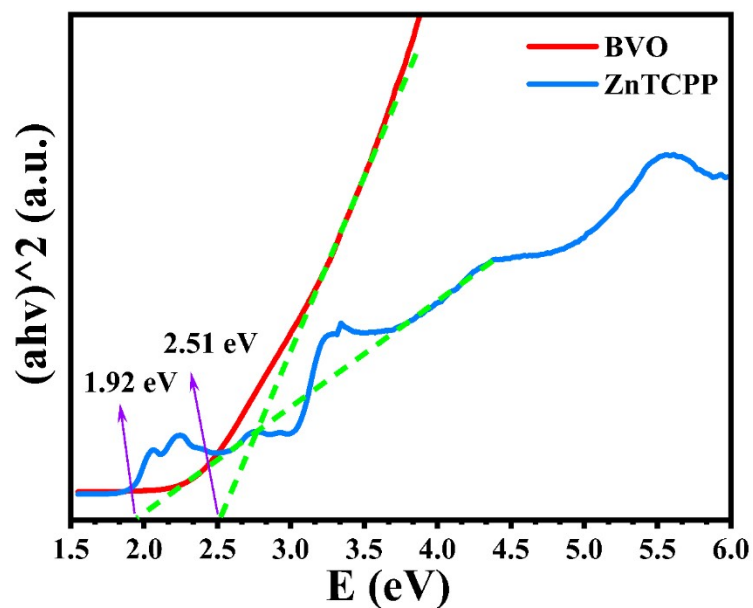


Figure S5. The plot of $(ah\nu)^2$ versus energy for the band gap energy of BiVO_4 and ZnTCPP samples.

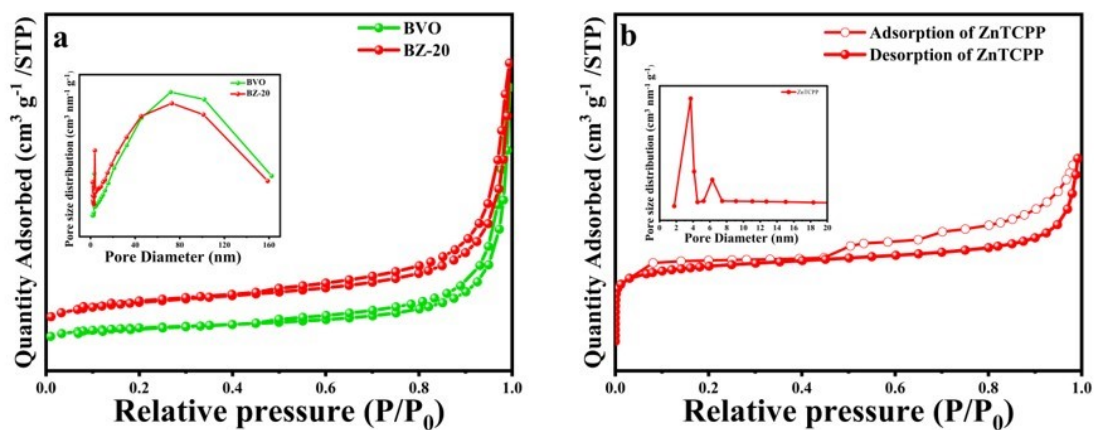


Figure S6. N_2 adsorption-desorption isotherms and corresponding pore size distributions of (a) BVO and BZ-20 and (b) ZnTCPP samples.

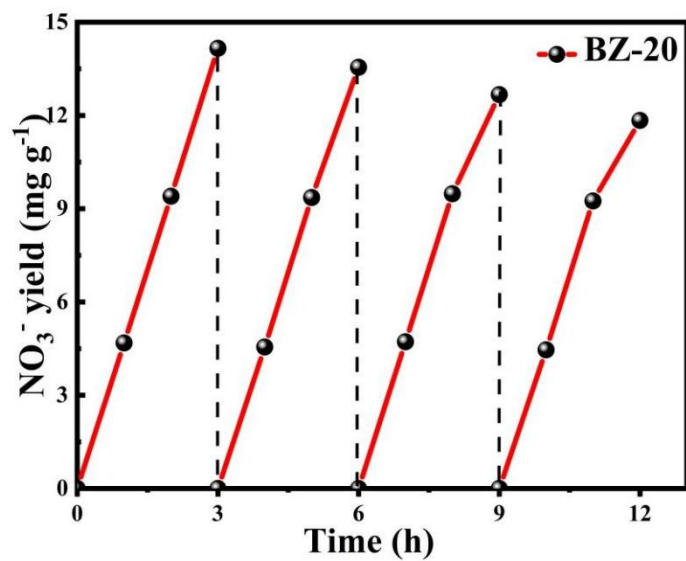


Figure S7. Stability of photocatalytic NO₃⁻ production over BZ-20 sample.

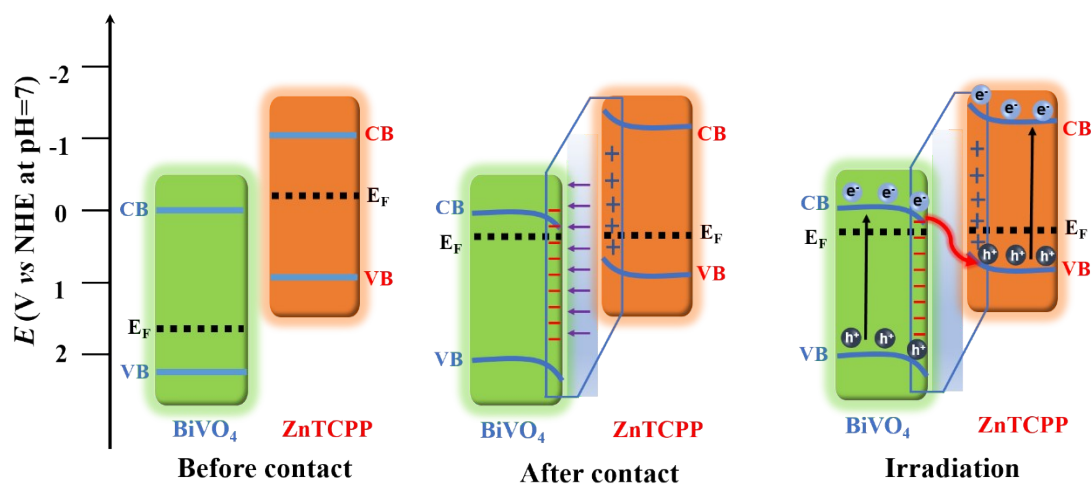


Figure S8. Schematic diagram for band structure of BiVO₄ and ZnTCPP before contact

(a), after contact (b) and the light-induced charge transfer from BiVO₄ to ZnTCPP (c).

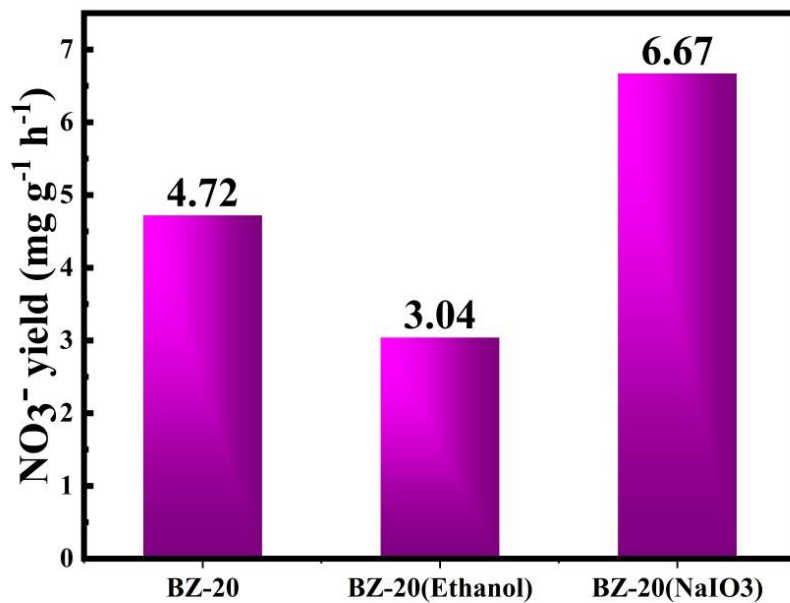


Figure S9. The control experiments that nitrate formation under different conditions on BZ-20 sample.

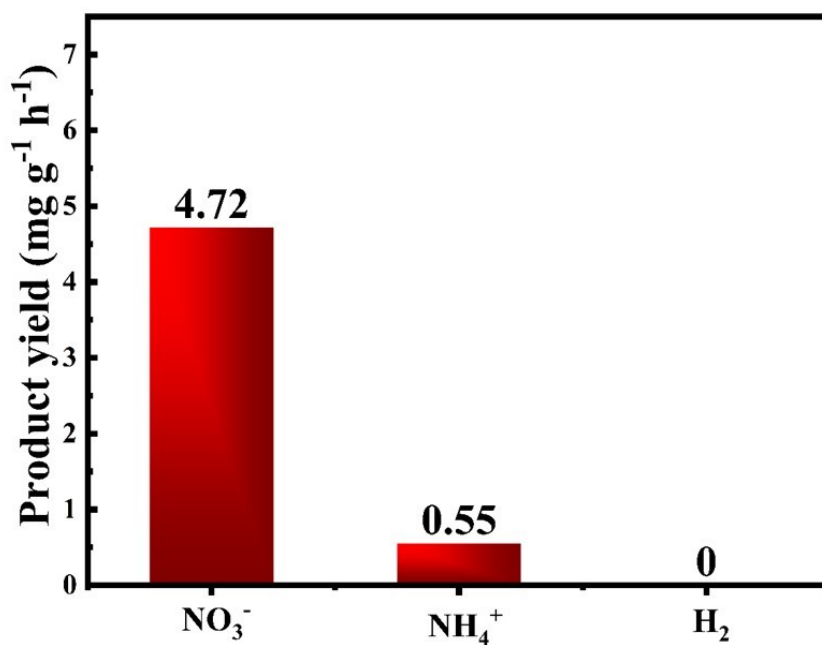


Figure S10. The photocatalytic H₂, NH₃ and NO₃⁻ production rate over BZ-20 sample.